# GREEN SYNTHESIS, CHARACTERIZATION, PHOTOCATALYTIC ACTIVITY OF ZnO/$TiO_2$ NANOCOMPOSITE FROM *Carica papaya* LEAVES

Safira Salsabilla, Dina Kartika Maharani*
Chemistry Department, Faculty of Mathematics and Natural Sciences, Universitas Negeri Surabaya, Jl. Ketintang, Surabaya 60231, East Java, Indonesia
*Email: dinakartika@unesa.ac.id

*Received 01 March 2023*
*Accepted 03 May 2023*

**Abstract**

This study aims to synthesize a ZnO/$TiO_2$ (ZT) nanocomposite from *Carica papaya* leaf extract and evaluate its photocatalytic activity. The ZT nanocomposite was prepared using the sol-gel method with ZnO/$TiO_2$ 4-gram (ZT4) concentration variations and ZnO/$TiO_2$ 6-gram (ZT6). Methylene Blue (MB) was used as a model dye to test its photocatalytic properties. The trend for most activity is shown by ZT4 UV light 40 mg and ZT6 UV light (60 mg), which is 87%. Characterization of ZnO/$TiO_2$ (ZT) nanocomposite using FTIR and XRD The ZT4 nanocomposite had an average crystallite size of approximately 12 nm and crystallinity percentage of 92%, whereas the ZT6 nanocomposite had an average crystallite size of approximately 6 nm and crystallinity percentage of 97%. FTIR resulted in some group C=C stretching alkene, C-H stretching vibrations of an aromatic aldehyde, and O-H stretching of alcohols and Zn-Ti-O in the fingerprint region 393.48 $cm^{-1}$ to 987.55 $cm^{-1}$ for ZT4 and in the fingerprint region 401.19 $cm^{-1}$ to 864.11 $cm^{-1}$ for ZT6.

***Keywords****: concentration, photocatalytic, UV, ZnO/$TiO_2$ nanocomposite*

## Introduction

The challenge of processing wastewater grows as more contaminants are added due to rising industrialization and urbanization in emerging countries. Globally, an estimated 700,000 tons of textile dyes are released into the environment annually because of industrial effluent discharge. Therefore, a suitable, environmentally friendly technology is needed to address these issues and be helpful for water disinfection(Li et al., 2017; Sethi & Sakthivel, 2017; Soto-Robles et al., 2021). Advanced oxidation procedures are becoming increasingly common because organic pollutants can be transformed into simple byproducts ($CO_2$ and $H_2O$). Photocatalysis has evolved into a powerful green method to generate $H_2$ and sanitize the environment. (Athira et al., 2020; Nabi et al., 2021).

The creation of multifunctional innovative values in standard materials has recently attracted much attention(Choi et al., 2017; Otitoju, Ahmad, and Ooi, 2017). Inorganic transition metal oxides, such as Ag, Au, Cu, CuO, ZnO, $TiO_2$, and $SnO_2$ may yield nanomaterials with vital applications. (Kaur *et al.*, 2019). Owing to the characteristics of $TiO_2$ and other metal oxides, the synthesis of $TiO_2$-metal oxide nanocomposites has attracted much interest for producing active photocatalysts. ZnO is a metal oxide that can be combined with $TiO_2$ to create a robust photocatalyst for the breakdown of organic contaminants. The nanocomposite system exhibited enhanced chemical reactivity, stability, and efficacy in eliminating the trapped centers present on the surface of ZnO, which are responsible for charge

recombination. (Ali *et al.*, 2021; Saeed *et al.*, 2021).

Nanostructured materials have attracted considerable interest in many sectors owing to their unique physicochemical properties. Reducing the particle size of nanocomposite materials results in a high surface-to-volume ratio, affecting their exciting features such as catalytic activity, optical absorption, and electrical capabilities(Rathnasamy *et al.*, 2017). Many techniques, including hydrothermal, precipitation, RF magnetron sputtering, sol-gel, and Taguchi approaches have been developed to create nanocomposites(Chi et al., 2017; Li et al., 2017; Taran, Rad, and Alavi, 2018; Suganthi, Thangavel and Kannan, 2020; Rusman et al., 2021). Moreover, using plant extracts, the green synthesis techniques used to create metal oxide nanoparticles are advantageous and environmentally safe (Ahmad, Jaiswal, and Soni, 2020).

The crystalline $ZnO/TiO_2$ nanocomposite has been successfully synthesized in a few attempts using leaf extract Recently, *Hibiscus subdariffa* leaves extract has had high potential as a photocatalyst agent (Suganthi, Thangavel, and Kannan, 2020); *verum* leaves significantly improve photocatalytic degradation for aqueous organic dye pollutants(Gowthaman *et al.*, 2022).

In developing with other studies, this work concentrated on fabricating ZnO-$TiO_2$ composite in nano size from *Carica papaya* leaf extract by adjusting the $TiO_2$ content in ZnO and examining its photocatalytic capability using methylene blue (MB) dye. The nanoparticles were characterized using UV-visible spectrophotometry, X-ray diffraction (XRD), and Fourier transform infrared (FTIR) spectroscopy.

## Research Methods

### *Materials*

Carica papaya (CP) leaves were utilized in this study; they were collected in the Sidoarjo area of East Java, Indonesia. Zinc acetate dihydrate ($Zn(CH_3COO)_2{\cdot}2H_2O$) (Merck 99,5%), titanium dioxide ($TiO_2$) (ROFA 98%), sodium hydroxide (NaOH) pellets (Merck), aqua demineralized and methylene blue (MB) 0,1%.

### *Instrumentation*

The equipment in this research was glassware, magnetic stirrer, oven, furnaces, UV-Vis Shimadzu 1800, X-ray diffraction (XRD) Shimadzu XRD-7000S, FTIR spectrophotometer 8201PC Shimadzu, UV box with UV light (LED @ 8 watts, two pieces), and a stopwatch.

### *Procedure*

The $Zn/TiO_2$ nanocomposite used in this study was synthesized using the sol-gel technique and derived from the extract of *Carica papaya* (CP) leaves.

1) Preparation of CP leaves extract and synthesis of $Zn/TiO_2$ nanocomposite

   The CP leaves underwent multiple rounds of washing with distilled water to eliminate any extraneous dirt particles and grimes. Subsequently, the leaves were left to air dry for one week at room temperature. The blended leaves were subsequently passed through a 100-mesh sieve to ensure uniformity. The experimental procedure involved agitation of 5 g of CP leaf powder in 100 mL of distilled water at a temperature of 80 °C for 20 min. The resulting mixture was filtered using Whatman No.1 paper filter.(Rathnasamy *et al.*, 2017). The filtrate was then used for the synthesis of $ZnO/TiO_2$.

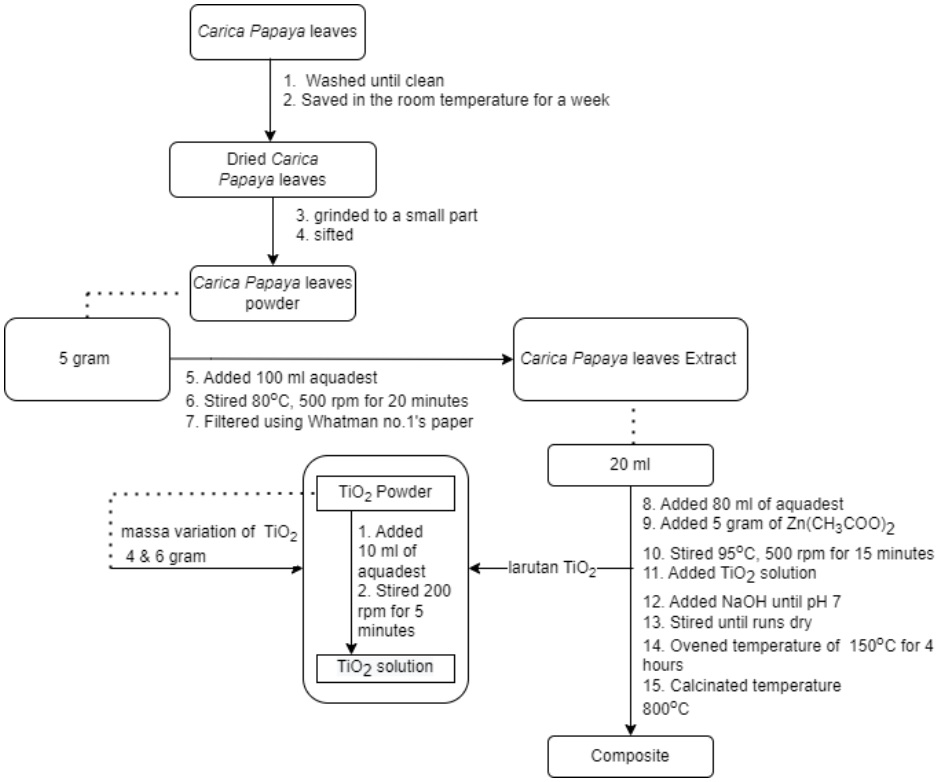


**Figure 1.** The procedure of ZT synthesis from *Carica papaya* leaves

The experimental procedure involved a combination of 5 g of Zn (Zn $(CH_3COO)_2{\cdot}2H_2O$), 80 mL of distilled water, and 20 mL of filtrate CP leaf extract. The mixture was stirred at 95°C at a rate of 500 rpm. Following a 15-minute heating period, a solution of $TiO_2$ was introduced into a solution of ZnO. The $TiO_2$ solution was prepared by homogenizing 4 and 6 g of $TiO_2$ powder with 10 ml of distilled water for 5 min at 200 rpm using a magnetic stirrer. Sodium hydroxide (NaOH) was incrementally added to the mixture with heating and stirring until a pH of 7 was achieved. The specimens were subjected to evaporation at 150°C for 4 h, followed by calcination at 800°C for 4 h, resulting in the production of $ZnO/TiO_2$ powder(Rusman *et al.*, 2021). A synthesis flowchart for the $ZnO/TiO_2$ (ZT) nanocomposite is shown in Figure 1. The corresponding chemical reactions to produce the $ZnO/TiO_2$ (ZT) nanocomposites are summarized in Eq. (1) and (6), respectively(Ali *et al.*, 2021).

$$Zn\ (CH_3COO)_2.2H_2O + 2NaOH \rightarrow ZnO + 2NaCH_3COO + H_2O \quad (1)$$

$$\{(CH_3)\ (CH_3)\ (CH_3)_2\}_4 + 4H_2O \rightarrow Ti\ (OH)_4 + 4HOCH(CH_3)_2 \quad (2)$$

$$Ti(OH)_4 + Ti(OH)_4 \rightarrow (OH)_3Ti - O - Ti(OH)_3 \quad (3)$$

$$(OH)_3\,Ti - O - Ti(OH)_3 \rightarrow 2TiO_2 + 3H_2O \quad (4)$$

$$\{(CH_3)\ (CH_3)\ (CH_3)_2\}_4 + 2H_2O \rightarrow TiO_2 + 4HOCH(CH_3)_2 \quad (5)$$

$$ZnO + TiO_2 \rightarrow ZnO/TiO_2 \quad (6)$$

2) Characterization

The powder was characterized by X-ray diffraction spectroscopy, Fourier transform infrared spectroscopy (FTIR), and UV-vis spectrophotometry. X-ray diffraction (XRD) spectroscopy can be used to determine the structure and crystallite size of materials by applying the Debye-Scherrer formula. (Shimadzu 700). Fourier Transform Infrared Spectroscopy (IRPrestige-21 (Shimadzu Corp.)) was used to conduct optical and functional group analyses of the samples. A UV-Vis spectrophotometer was used to examine the photocatalytic performance of MB (Shimadzu UV-Vis Spectrophotometer UV-1800). The powder was characterized by X-ray diffraction spectroscopy, Fourier transform infrared spectroscopy, and UV-vis spectrophotometry. X-ray diffraction (XRD) spectroscopy can be utilized to determine the structure and crystallite size of materials using the application of the Debye-Scherrer formula. (Shimadzu 700). Fourier Transform Infrared Spectroscopy (IRPrestige-21 (Shimadzu Corp.)) was used to conduct optical and functional group analyses of the samples. A UV-Vis spectrophotometer was used to examine the photocatalytic efficacy of MB (Shimadzu UV-Vis Spectrophotometer UV-1800).

3) Photocatalytic activities

The degradation of MB dye by ZnO-TiO2 nanocomposites under both light and dark conditions was used to study their photocatalytic properties. UV light from a lamp with a 100–280 nm wavelength and power output of 16 W. The mixture was first exposed to UV radiation for two hours with stirring. Zinc oxide-titanium dioxide (ZnO-TiO2) at concentrations of 20, 40, 60, 80, and 100 mg was blended with 10 mL of Methylene Blue (MB) dye at a concentration of ten parts per million (ppm). The pH of the samples was adjusted to 7 using 0.1 M NaOH upon withdrawal at intermediate time intervals. The mixture was initially placed under low-light conditions and stirred for a duration of two hours. A UV-Vis spectrophotometer is capable of measuring absorbance within the wavelength range of 400–800 nm. (Shimadzu UV-Vis Spectrophotometer UV-1800).

## Results and Discussion

*XRD analysis*

The XRD pattern of $ZnO/TiO_2$ is shown in Figure 2. The XRD patterns of the composite system demonstrate the presence of ZnO and TiO reflections. (Rajendar et al., 2017). The distinct diffraction peaks at 2θ for $TiO_2$ in ZT4 based on the diffraction pattern corresponding to the standard Joint Committee on Powder Diffraction Standards JCPDS No. 21-1272 (Saeed *et al.*, 2021) were 28.78°and 32.46°. Moreover, the distinct diffraction peaks at 2θ for $TiO_2$ in ZT6 were 28.7°, 32.6°, 33.3°, 40.4°, 43.36°, 44.98°, 46.22°. As the wt% of Ti in ZnO increased, the peak intensities of the $TiO_2$ anatase phase increased(Haghighatzadeh *et al.*, 2019). Similarly, the diffraction peaks of ZnO in ZT4 based on the diffraction pattern corresponding to the standard Joint Committee on Powder Diffraction Standards JCPDS No. 89-1397 (Ramesh, Anbuvannan and Viruthagiri, 2015) were 31.8°, 34.34°, 36.2°, 47.5°, 56.58°, 62.86°, 67.94° and for ZT6 at 31.88°, 34.18°, 36.04°, 36.74°, 52.52°, 56.42°, 64.32°, and 66.2°, respectively. The average grain size of the sample was determined using Scherrer equation (1).

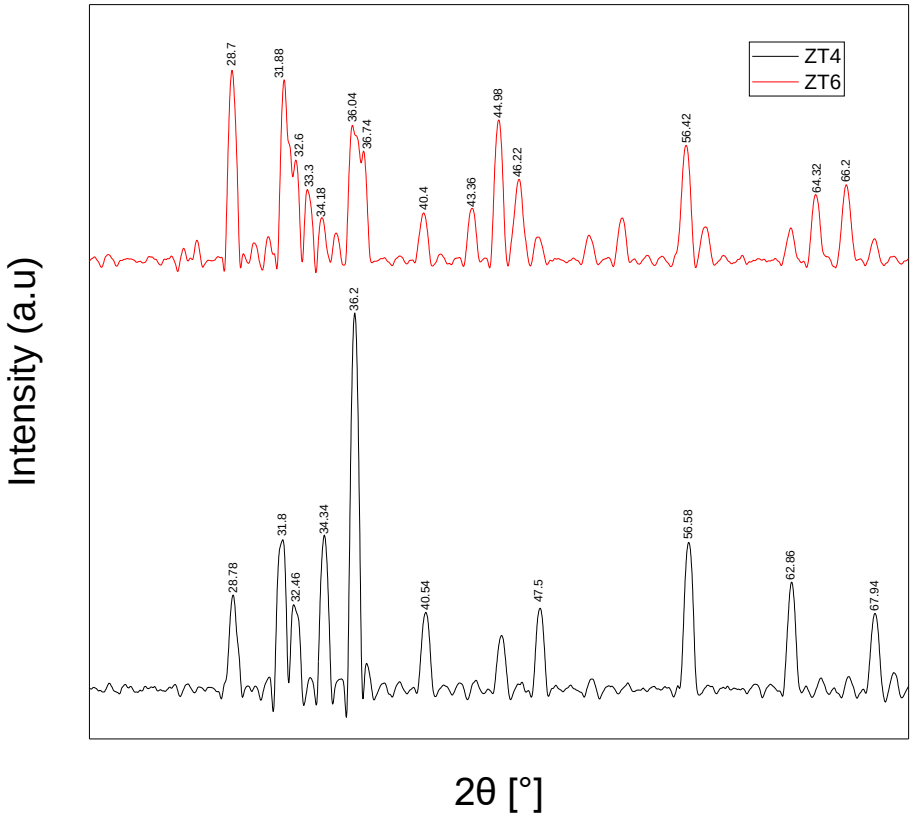


**Figure 2.** XRD analysis result

$$D = \frac{K\,\lambda}{\beta\,Cos\,\theta}\ \text{Å} \qquad (1)$$

Where D is the average crystallite size (Å), K is the shape factor (0.9), λ is the wavelength of the X-ray (1.5406 Å) Cu Kα radiation, θ is the Bragg angle, and β is the corrected line broadening of the nanocomposite. The size of the NPs ranged from 10 nm to 100 nm(Rajendra et al., 2017). The mean particle sizes of ZT4 and ZT6 were 12 and 6 nm, respectively, with a crystallinity percentage of 92% for ZT4 and a crystallinity percentage of 97% for ZT6.

*FTIR analysis*

The surface of the ZnO /$TiO_2$ nanocomposite was studied using FTIR spectroscopy. Figure 3 shows the FTIR spectra of ZT4 and ZT6. Multiple bands between 4000 and 500 $cm^{-1}$ may be seen for all samples. In the fingerprint region (below 1000 $cm^{-1}$), metal oxides typically exhibit absorption bands caused by interatomic vibrations. Zn-Ti, Ti-O, and Zn-O stretching bonds could account for a band detected at wavelengths less than 600 $cm^{-1}$ (Ahmed & Ikram, 2017; Sethi and Sakthivel, 2017). The FTIR spectrum of ZnO/TiO2 synthesized through green methods indicates the presence of an absorption band in the fingerprint region at 393.48 cm-1 for ZT;4 and at 401.19 cm-1 for ZT6, which corresponds to the stretching mode of Zn-Ti-O. It is observed that the bands are at 1635.64 (C=C stretching alkene), 2931.8 (C-H stretching vibrations of an aromatic aldehyde), 3448.72 in ZT4, and 3433.29 in ZT6 (O-H stretching of alcohols). The bands at 3420 and 1650 $cm^{-1}$ were assigned to the stretching and bending vibrations of $H_2O$ adsorbed on the surface of the solid in this spectrum and the ZnO-$TiO_2$ materials developed in this work.

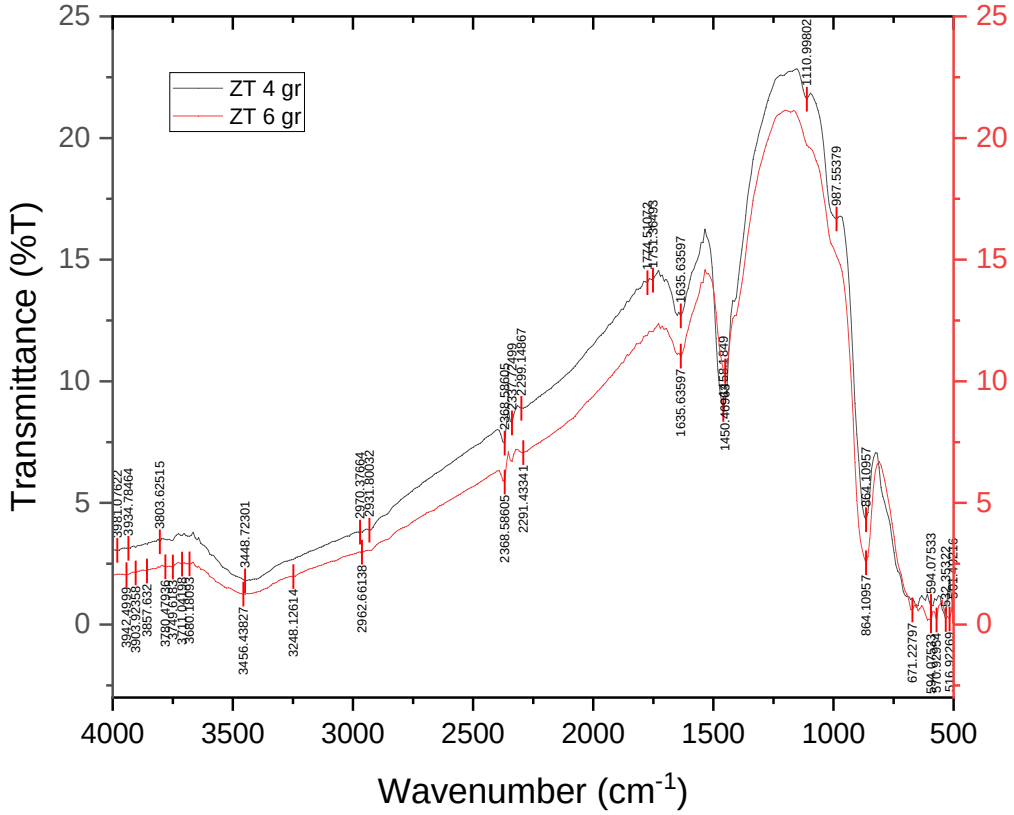


**Figure 3.** FTIR spectrum of ZT4 and ZT6

*Photocatalytic activities*

The photodegradation ability of methylene blue (MB) dye in the presence of UV light and non-UV (dark condition) light was used to evaluate the photocatalytic performance of the nanocomposites. After 120 min, the samples were collected and mixed with various nanocomposite concentrations to determine the degree of dye degradation. Using UV–Vis spectrometry, all synthetic light absorption characteristics were displayed in the 200-800 nm wavelength range.

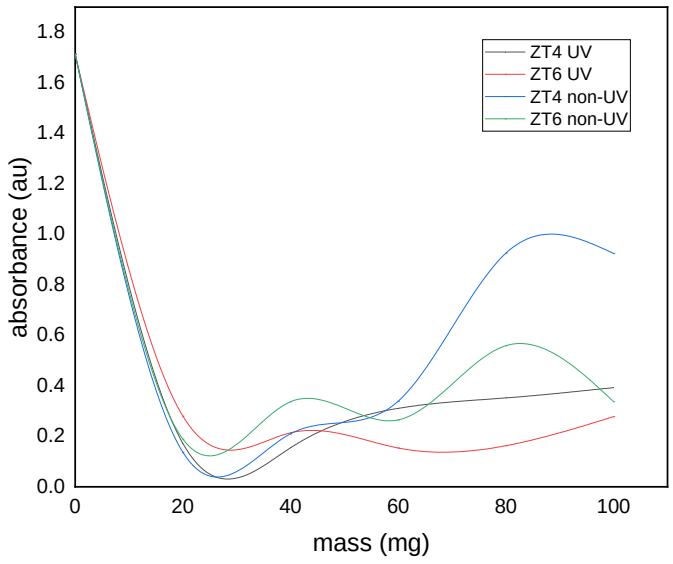


**Figure 4.** Absorption spectra ZT4 and ZT6 in the light and dark conditions

Figure 4 depicts the absorption spectra of MB dye in the presence of ZT4 and ZT6 nanocomposites with and without UV radiation (dark conditions) at concentrations of 0, 20, 40, 60, 80, and 100 mg. The absorption rate decreased as the mass increased.

The decolorization of aqueous MB solutions was used to test the photocatalytic performance of the pristine ZnO/$TiO_2$ nanocomposites. Solutions with a dye concentration of 10 ppm and pH of 8 provided the best conditions for validating the decolorization efficiency. Figure 5 shows the data obtained. The produced photocatalysts displayed moderate to good photocatalytic activity for the removal of MB from aqueous solutions. The chromophores contained within the pigment that give the dye its specific color may break down with time, which may lead to the color of the dye becoming less vibrant.

(**a**) (**b**)

**Figure 5.** Degradation's appearance of MB, (a) ZT4, (b) ZT6

UV irradiation of light shining over the produced catalyst encourages the injection of extra electrons into the conduction band of $TiO_2$ through a mechanism known as surface phonon resonance, which contributes to the generation of free radicals, and (Kandregula et al., 2015). TiO2 is incorporated into ZnO to stop recombination. The recombination properties of ZnO were suppressed, and a large amount of the element was made available on the surface of the nanocomposite owing to the transfer of electrons from the conduction band to $TiO_2$'s conduction band and holes from TiO2's valence band to the valence band of ZnO(Ali *et al.*, 2021; Saeed *et al.*, 2021).

**Table 1.** Calculation of percent degradation

| | mass | Abs | C | % Degradation | | mass | Abs | C | % Degradation |
|---|---|---|---|---|---|---|---|---|---|
| UV ZT4 | 0 | 1.714 | 8.65 | 13.52 | non UV ZT4 | 0 | 1.714 | 8.65 | 13.52 |
| | 20 | 0.172 | 1.41 | 85.92 | | 20 | 0.137 | 1.24 | 87.56 |
| | 40 | 0.155 | 1.33 | 86.71 | | 40 | 0.21 | 1.59 | 84.13 |
| | 60 | 0.311 | 2.06 | 79.39 | | 60 | 0.339 | 2.19 | 78.08 |
| | 80 | 0.352 | 2.25 | 77.46 | | 80 | 0.926 | 4.95 | 50.52 |
| | 100 | 0.393 | 2.45 | 75.54 | | 100 | 0.924 | 4.94 | 50.61 |
| UV ZT6 | 0 | 1.714 | 8.65 | 13.52 | non UV ZT6 | 0 | 1.714 | 8.65 | 13.52 |
| | 20 | 0.28 | 1.92 | 80.85 | | 20 | 0.189 | 1.49 | 85.12 |
| | 40 | 0.214 | 1.61 | 83.94 | | 40 | 0.337 | 2.18 | 78.17 |
| | 60 | 0.154 | 1.32 | 86.76 | | 60 | 0.265 | 1.85 | 81.55 |
| | 80 | 0.163 | 1.37 | 86.34 | | 80 | 0.559 | 3.23 | 67.75 |
| | 100 | 0.278 | 1.91 | 80.94 | | 100 | 0.337 | 2.18 | 78.17 |

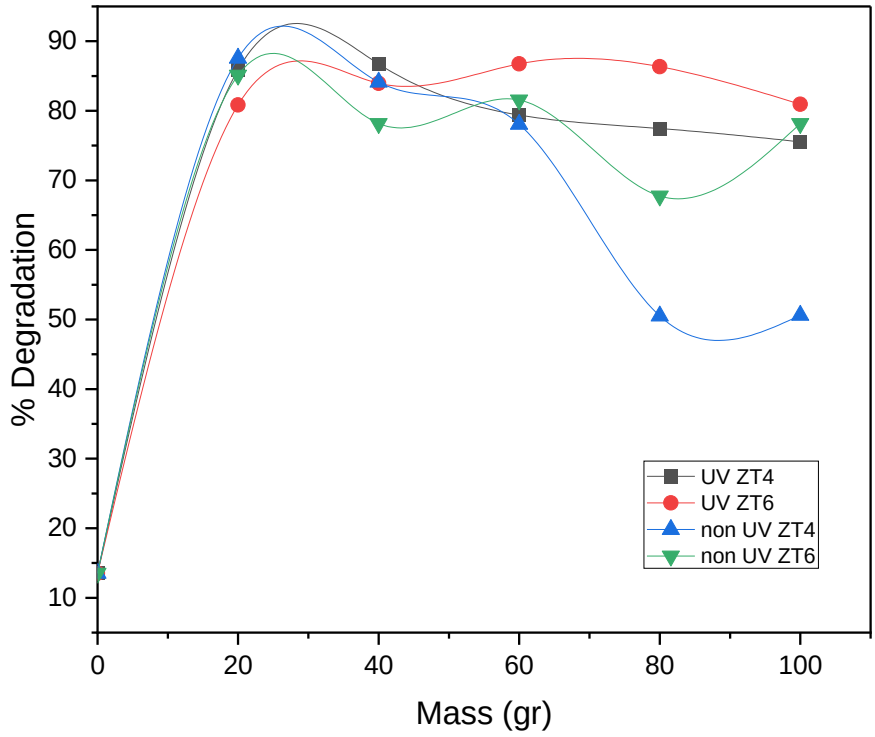


**Figure 6.** Percent degradation's graph

Table 1 and Figure 6 depict the measured photoactivities of the samples. Photocatalytic tests showed that the inclusion of a ZT4 and ZT6 nanocomposite resulted in maximum photodegradation efficiency. This photocatalytic activity can be explained by the considerable presence of a $TiO_2$-related crystalline structure surrounding the ZnO core, which significantly reduces the band gap (improves photocatalytic). The results of the photocatalytic experiments showed that the ZnO/$TiO_2$ nanocomposite significantly enhanced photodegradation, with the photocatalytic peak activity trending toward ZT4 UV light at 40 mg and ZT6 UV light at 60 mg being 87%.

Furthermore, ZT4 and ZT6 were less effective in degrading at lower $TiO_2$ concentrations(Rajendar et al., 2017). Therefore, the degradation efficiency of the nanocomposites increased as the $TiO_2$ level increased. The increased reaction rate was mostly caused by the smaller particle size, which reduced the resistance to charge transfer and facilitated the migration of electrons to the surface(Parida *et al.*, 2010). In addition to particle size, improved crystallinity was also cited by Gaurav K. Upad-hyay as a factor in regulating the photocatalytic activity of nanoparticles(Chi *et al.*, 2017). ZT6 demonstrated superior photocatalytic activity owing to its small particle size (6 nm) and the highest degree of crystallinity (97%).

## Conclusions

ZnO/$TiO_2$ (ZT) nanocomposites from *Carica papaya* leaf extract were successfully synthesized using a green synthesis method with varying $TiO_2$ mass. The ZnO/$TiO_2$ (ZT) nanocomposites were also analyzed using FTIR spectrophotometry, X-ray diffraction (XRD), and UV-Vis S spectrophotometer.

Photocatalytic activities show that the inclusion of a ZT4 and ZT6 nanocomposite results in a maximum photodegradation efficiency of 87% for 40 mg ZT4 and 60 mg ZT6 under UV light. However, ZT6 demonstrated superior crystallinity, 5% higher than that of ZT4. More research is needed to address water contamination and

environmental pollution because the decolorization of MB aqueous solutions cannot represent environmental conditions.

## References


Ali, M.M. *et al.*, 2021. Nano synthesis of ZnO–$TiO_2$ composites by sol-gel method and evaluation of their antibacterial, optical and photocatalytic activities, *Results in Materials*, 11.

Athira, T.K. *et al.*, 2020. Evaluation of photocatalytic activity of commercial red phosphorus towards the disinfection of E. coli and reduction of Cr (VI) under direct sunlight, *Materials Research Express*, 7(10).

Chi, C.-Y. *et al.*, 2017. Construction of $TiO_2$ /ZnO Heterostructure for Photocatalytic Application.

Choi, D. *et al.*, 2017. Facile and cost-effective fabrication of patternable superhydrophobic surfaces via salt dissolution assisted etching, *Applied Surface Science*, 393, pp. 449–456.

Gowthaman, K. *et al.*, 2022. Design and synthesis of $TiO_2$/ZnO nanocomposite with enhanced oxygen vacancy: Better photocatalytic removal of MB dye under visible light-driven condition, *Inorganic Chemistry Communications*, 146, p. 110197.

Haghighatzadeh, A. *et al.*, 2019. Improved photocatalytic activity of ZnO-$TiO_2$ nanocomposite catalysts by modulating $TiO_2$ thickness, *Materials Research Express*, 6(11).

Kandregula, G. *et al.*, 2015. Green Synthesis of $TiO_2$ Nanoparticles Using Aloe Vera Extract Green Synthesis of TiO 2 Nanoparticles Using Aloe Vera Extract, *International Journal of Advanced Research in Physical Science (IJARPS)*.

Kaur, H. *et al.*, 2019. Expanding horizon: Green synthesis of $TiO_2$ nanoparticles using Carica papaya leaves for photocatalysis application, *Materials Research Express*, 6(9).

Li, X. *et al.*, 2017. Novel ZnO-$TiO_2$ nanocomposite arrays on Ti fabric for enhanced photocatalytic application, *Journal of Molecular Structure*, 1148, pp. 347–355.

Nabi, G. *et al.*, 2021. Green synthesis of spherical $TiO_2$ nanoparticles using Citrus Limetta extract: Excellent photocatalytic water decontamination agent for RhB dye, *Inorganic Chemistry Communications*, 129.

Otitoju, T.A., Ahmad, A.L. and Ooi, B.S., 2017. Superhydrophilic (superwetting) surfaces: A review on fabrication and application, *Journal of Industrial and Engineering Chemistry*. Korean Society of Industrial Engineering Chemistry, pp. 19–40.

Parida, K.M. *et al.*, 2010. 'Fabrication of nanocrystalline LaFeO3: An efficient sol–gel auto-combustion assisted visible light responsive photocatalyst for water decomposition, *International Journal of Hydrogen Energy*, 35(22), pp. 12161–12168.

Rajendar, V. *et al.* Synthesis, Characterization, and Photocatalytic Behaviour of Nanocrystalline ZnO/TiO2 Nanocomposite, *Journal of Ovonic Research.*

Ramesh, M., Anbuvannan, M. and Viruthagiri, G., 2015. Green synthesis of ZnO nanoparticles using Solanum nigrum leaf extract and their antibacterial activity, *Spectrochimica Acta - Part A: Molecular and Biomolecular Spectroscopy*, 136(PB), pp. 864–870.

Rathnasamy, R. *et al.*, 2017. Green synthesis of ZnO nanoparticles using Carica papaya leaf extracts for photocatalytic and photovoltaic applications, *Journal of Materials Science: Materials in Electronics*, 28(14), pp. 10374–10381.

Rusman, E. *et al.*, 2021.Green Synthesis ZnO/$TiO_2$ for High Recyclability Rapid Sunlight Photodegradation Textile Dyes Applications.

Saeed, M. *et al.*, 2021. ZnO–$TiO_2$: Synthesis, characterization and evaluation of photo catalytic activity towards degradation of methyl orange, *Zeitschrift fur Physikalische Chemie*, 235(3), pp. 225–237.

Sethi, D. and Sakthivel, R., 2017. ZnO/$TiO_2$ composites for photocatalytic inactivation of Escherichia coli, *Journal of Photochemistry and Photobiology B: Biology*, 168, pp. 117–123.

Soto-Robles, C.A. *et al.*, 2021. Biosynthesis, characterization and photocatalytic activity of ZnO nanoparticles using extracts of Justicia spicigera for the degradation of methylene blue, *Journal of Molecular Structure*, 1225.

Suganthi, N., Thangavel, S. and Kannan, K., 2020. Hibiscus subdariffa leaf extract mediated 2-D fern-like ZnO/$TiO_2$ hierarchical nanoleaf for photocatalytic degradation', *FlatChem*, 24.

Taran, M., Rad, M. and Alavi, M., 2018. Biosynthesis of $TiO_2$ and ZnO nanoparticles by Halomonas elongata IBRC-M 10214 in different conditions of medium, *BioImpacts*, 8(2), pp. 81–89.